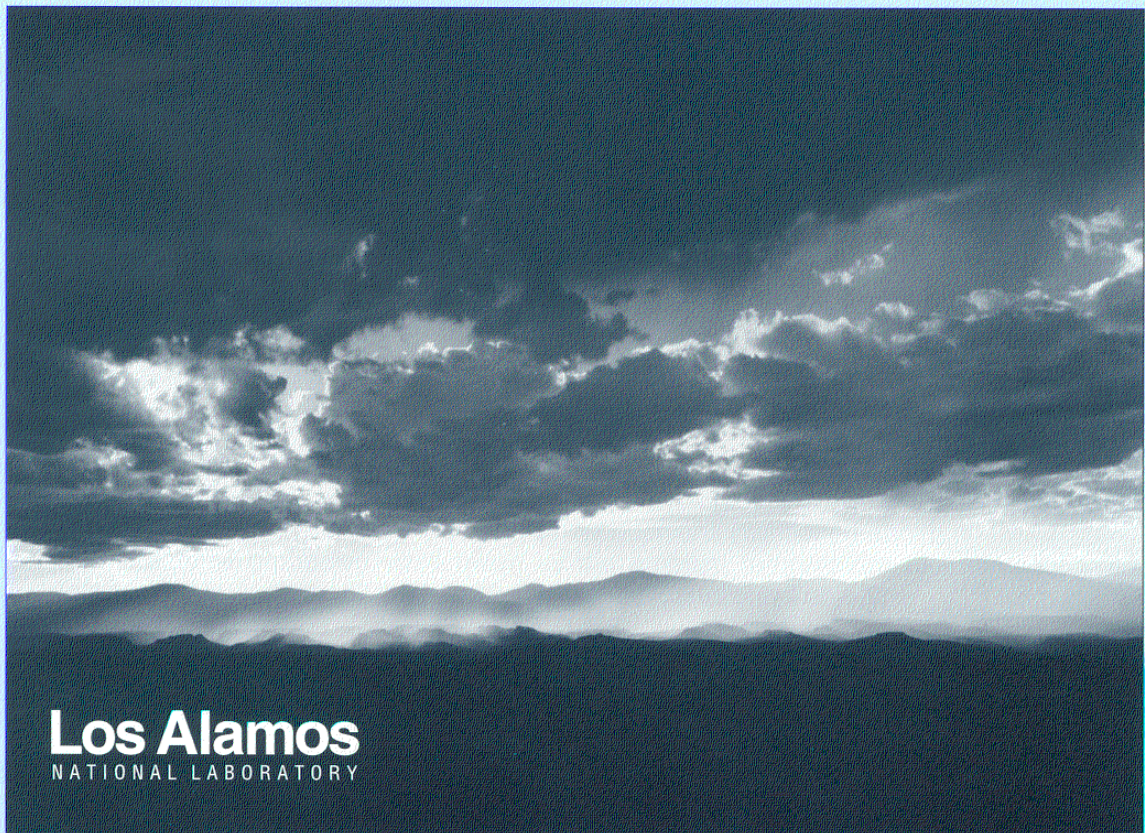


Title: RESONANT STRUCTURAL FREQUENCY ANALYSIS OF ARGONNE NATIONAL
LABORATORY 3-GAP, 350 MHz, $B_g = .36$ SPOKE RESONATOR CAVITY

Author(s): Richard P. LaFave

LANSCE-1

Submitted To: Informal Distribution - Internal and External



Los Alamos

NATIONAL LABORATORY

memorandum

LANSCE Division
Group LANSCE-1

To/MS: Dale Schrage, MS H817
From/MS: Richard LaFave, MS H817
Phone/FAX: 5-0029/5-2904
Symbol: LANSCE-1:00-78
Date: September 12, 2000
Email: rpl@lanl.gov

RR

***SUBJECT: Resonant Structural Frequency Analysis of
Argonne National Laboratory 3-gap, 350 MHz, $\beta_g = .36$ Spoke
Resonator Cavity***

Ref: R. LaFave to D. Schrage memo LANSCE-1:00-69, 'Structural Analysis of Argonne National Laboratory 3-gap, 350 MHz, $\beta_g = .36$ Spoke Resonator Cavity' dated August 14, 2000

Introduction:

As requested, the analysis summarized in the referenced memo has been expanded to include a determination of resonant structural frequencies of the Argonne National Laboratory 3-gap, 350 MHz, $\beta_g = .36$ spoke resonator cavity. This memo summarizes the model predictions for those resonant structural frequencies. The results shown in Table 2 summarize the model predictions for the various boundary conditions and geometries considered. Material properties were taken as the ambient temperature niobium properties listed in Table 3 of LA-UR # 99-5826.

Models:

Models of the 3-gap, 350 MHz, $\beta_g = .36$ spoke resonator have been constructed for COSMOS/M and represent the cavity geometry as defined in Argonne drawing EB-24003-X, dated February 28, 2000, which is reproduced in Figure 7. In addition to the geometry as defined in the drawing, variations in geometry were also considered. They were:

- a) The addition of an annular end wall stiffener.
- b) Changing the geometry of the radial end wall stiffeners to wrap around the outer diameter of the main body.

Figure 1 shows the cavity geometry as defined by Argonne drawing EB-24003-X, while Figure 2 shows the geometry with both of the additions mentioned above.

Material properties were taken as the ambient temperature niobium properties listed in Table 3 of LA-UR # 99-5826 and are reproduced in Table 1.

Table 1: Room Temperature Properties of Niobium

Property	Value	Units
Density, ρ	0.31	lb/in ³
Modulus, E	1.42X10 ⁷	lb/in ²
Yield Strength, σ_y	7000	lb/in ²
Poisson's Ratio, ν	0.38	none

The models were meshed with three and four node shell elements resulting in problems with between 55,000 and 65,000 degrees of freedom (DOF). Figure 3 shows the mesh generated when both of the additions mentioned above were included. Figure 4 shows the mesh for a cavity with no endwall stiffeners. Figure 5 shows a cutaway view that illustrates the internal configuration of the cavity.

Boundary Conditions:

Four sets of boundary conditions were considered for the models:

- A six DOF restraint. This represents the simplest set of constraints with the minimum number required to fix the model in space.
- Both end flanges fully restrained.
- Torsional restraint. This is an additional restraint that was used in addition to either of the previous sets to represent the restrictions that side flanges would generate.

Results and Discussion:

Results for each of the cases considered are tabulated in table 2. Figures 6a and 6b show results for case 37, mode 1, and represent a typical axial translation mode. Figure 6a is a displaced model plot while figure 6b is a cutaway side view of the model overlaid with an outline of the undeformed model. As can be seen in figure 6b both end flanges remain fixed while the body of the cavity moves along the beam axis. This particular mode is the lowest order mode for all torsionally restrained models. It should be noted that the scale presented in figures 6a and 6b are not representative of actual displacements, and so should not be interpreted as such.

Because of the variety of conditions represented in Table 2 some general comments are in order:

- Radial Endwall Stiffeners:** The presence of the radial endwall stiffeners increases the first mode frequency to a minimum of 114 Hz (case 34). This compares to a first mode frequency of only 34 Hz when no endwall stiffeners are present (case 42). This is a significant improvement.
- Annular Endwall Stiffener:** The addition of an annular endwall stiffener does not have a significant impact on the resonant structural frequencies (cases 38-41).
- Torsional Restraint:** The presence of a torsional restraint such as the restriction generated through the flanges on the outer diameter of the

main body, increases the first mode frequency to over 170 Hz when used in conjunction with radial endwall stiffeners (case 35).

Summary:

The structural analysis of the Argonne National Laboratory 3-gap, 350 MHz, $\beta_g=.36$ spoke resonator cavity discussed in the referenced memo has been expanded to include determination of resonant structural frequencies of the cavity. The results of these cases are presented in Table 2 and include cases to consider variations in structural constraints and changes in the configuration of the endwall stiffeners. The analysis indicates that the endwall stiffeners are necessary to increase resonant frequencies to over 100 Hz. In this configuration the structure is very stiff. The analysis also indicates that the presence or absence of an annular endwall stiffener has little effect on resonant frequencies.

Los Alamos National Laboratory
GROUP LANSCE-1

Table 2; Results from Analysis of ANL 350 MHz 3-Gap Spoke Resonator

Case Number	Boundary Conditions			Radial Endwall Stiffeners		Annular Endwall Stiffener	Wall Thick (mm)	F ₁ Mode Shape		F ₂ Mode Shape		F ₃ Mode Shape		F ₄ Mode Shape		F ₅ Mode Shape	
	6 DOF Restraint	Torsional Restraint	Fixed End Flanges	ANL EB-24003-X	Wrap Around Tips			F ₁ (Hz)	Mode Shape	F ₂ (Hz)	Mode Shape	F ₃ (Hz)	Mode Shape	F ₄ (Hz)	Mode Shape	F ₅ (Hz)	Mode Shape
						Yes	No										
34	X				X		X	114	Torsional	171	Trans/Axial	489	Trans/Vert	503	Trans/Lat	601	Rot/Pitch
35	X	X			X		X	171	Trans/Axial	380	Trans/Vert	503	Trans/Lat	616	Rot/Yaw	662	End/Drum
36			X		X		X	221	Torsional	291	Trans/Axial	613	Trans/Vert	613	Rot/Pitch	681	Rot/Yaw
37		X	X		X		X	292	Trans/Axial	499	Trans/Vert	613	Trans/Lat	681	CrossSect.	695	Trans/Vert
38	X				X		X	114	Torsional	181	Trans/Axial	491	Trans/Vert	504	Trans/Lat	602	Rot/Pitch
39	X	X			X		X	180	Trans/Axial	382	Trans/Vert	504	Trans/Lat	617	Rot/Yaw	669	End/Drum
40			X		X		X	224	Torsional	312	Trans/Axial	619	Trans/Vert	620	Rot/Pitch	685	CrossSect.
41		X	X		X		X	312	Trans/Axial	504	Trans/Vert	620	Trans/Lat	685	CrossSect.	697	Trans/Vert
42	X						X	34	Torsional	102	Trans/Axial	190	Trans/Vert	191	Trans/Lat	227	Rot/Pitch
43	X	X					X	103	Trans/Axial	148	Trans/Vert	191	Trans/Lat	231	Rot/Yaw	574	Rot/Pitch
44			X				X	56	Torsional	157	Trans/Axial	348	Trans/Vert	348	Trans/Lat	360	Rot/Pitch
45		X	X				X	157	Trans/Axial	266	Trans/Vert	347	Trans/Lat	361	Rot/Yaw	618	Rot/Pitch

FIGURE 1
ANL 350 MHZ 3-GAP SPOKE CAVITY
GEOMETRY PER ANL EB-24003-X

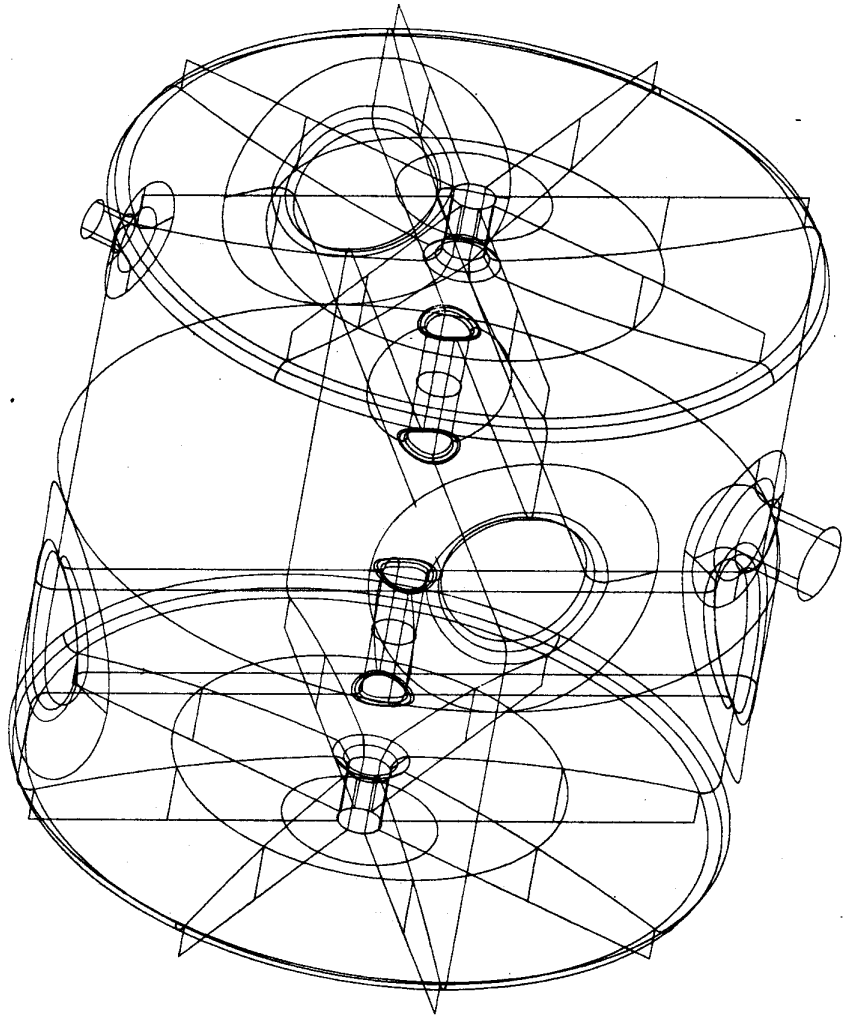


FIGURE 2
ANL 350 MHZ 3-GAP SPOKE CAVITY
WITH WRAP-AROUND RADIAL ENDWALL STIFFENERS
WITH ANNULAR ENDWALL STIFFENER

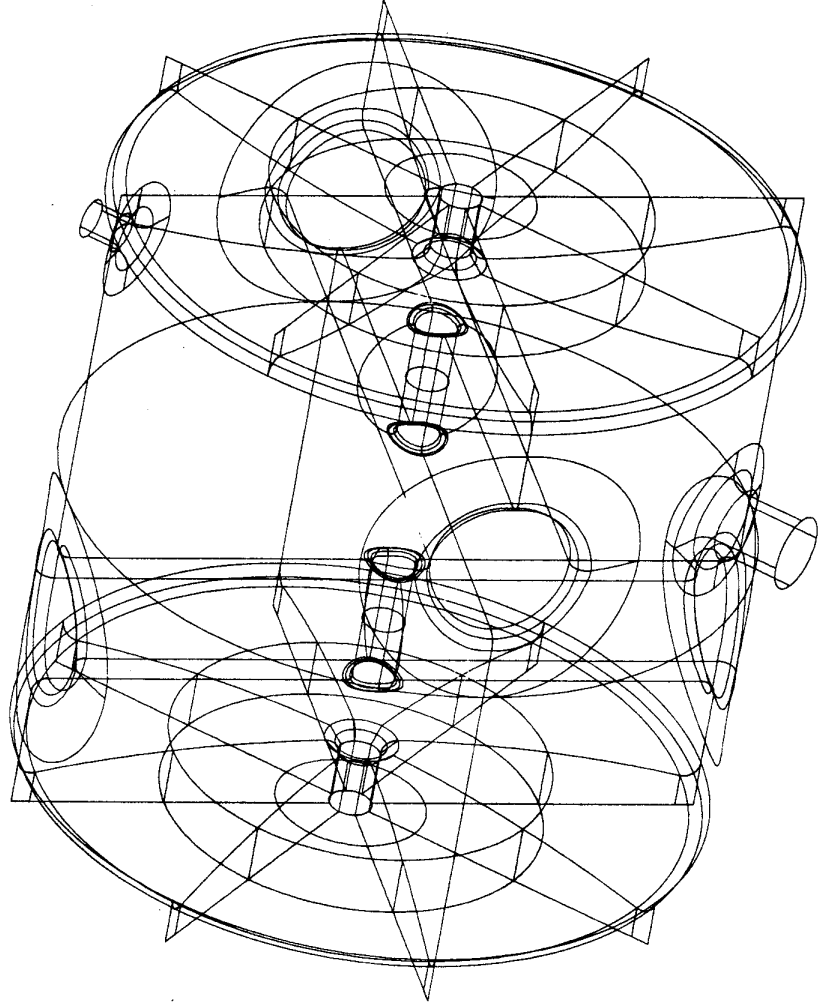


FIGURE 3
ANL 350 MHZ 3-GAP CAVITY ELEMENTS
WITH WRAP-AROUND RADIAL ENDWALL STIFFENERS
WITH ANNULAR ENDWALL STIFFENER

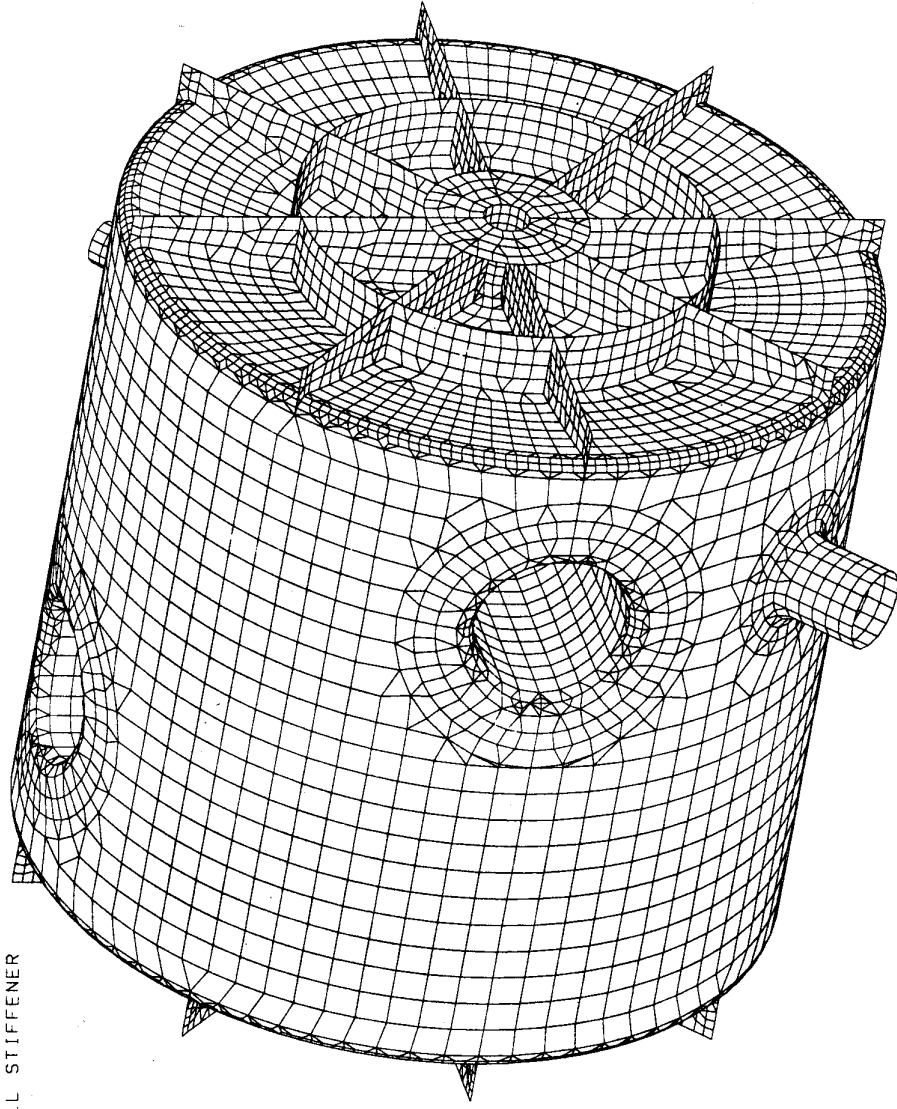


FIGURE 4
ANL 350 MHZ 3-GAP CAVITY ELEMENTS
NO STIFFENERS

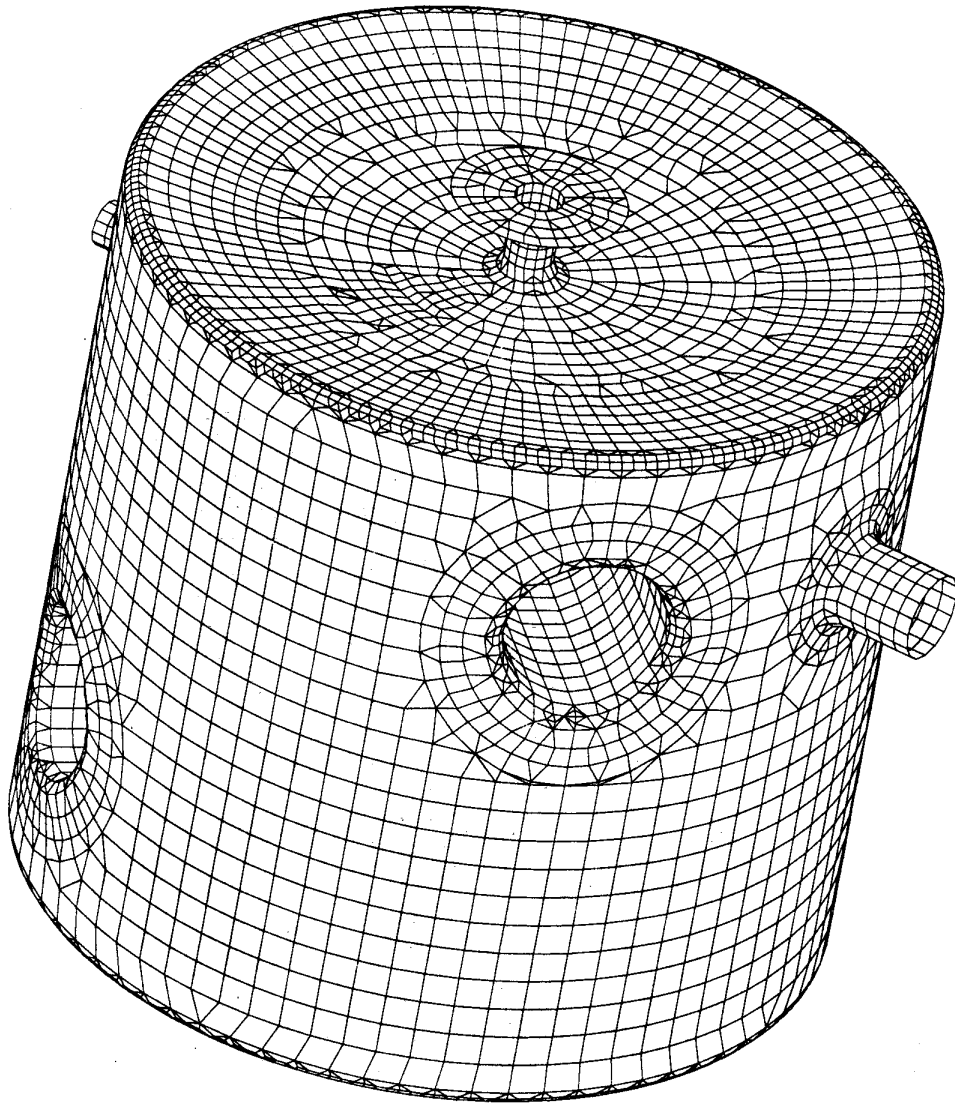
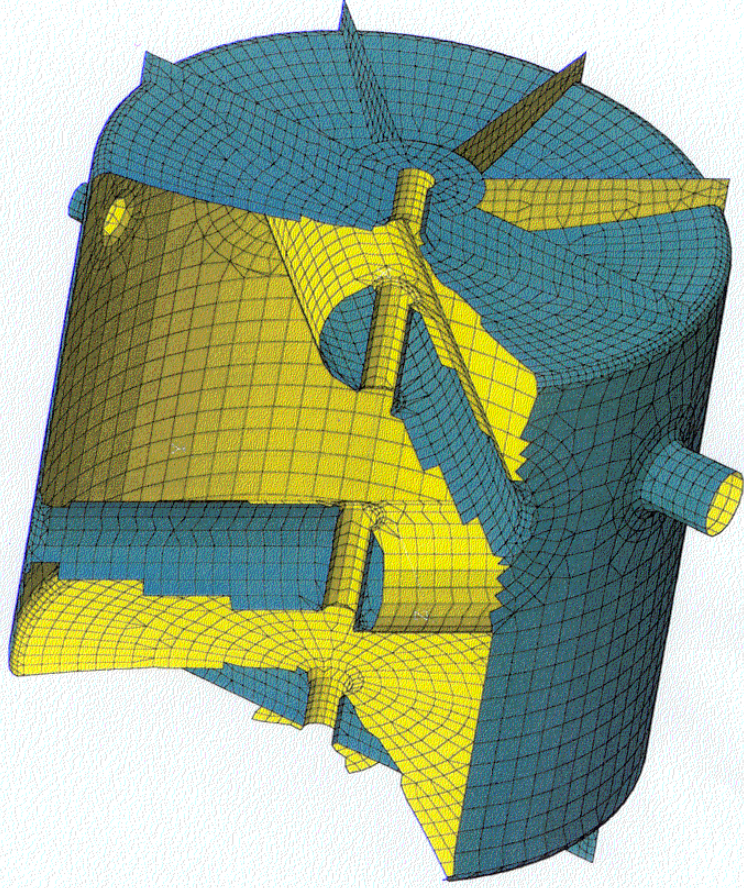


FIGURE 5
ANL 350 MHZ 3-GAP CAVITY ELEMENTS
CUTAWAY VIEW

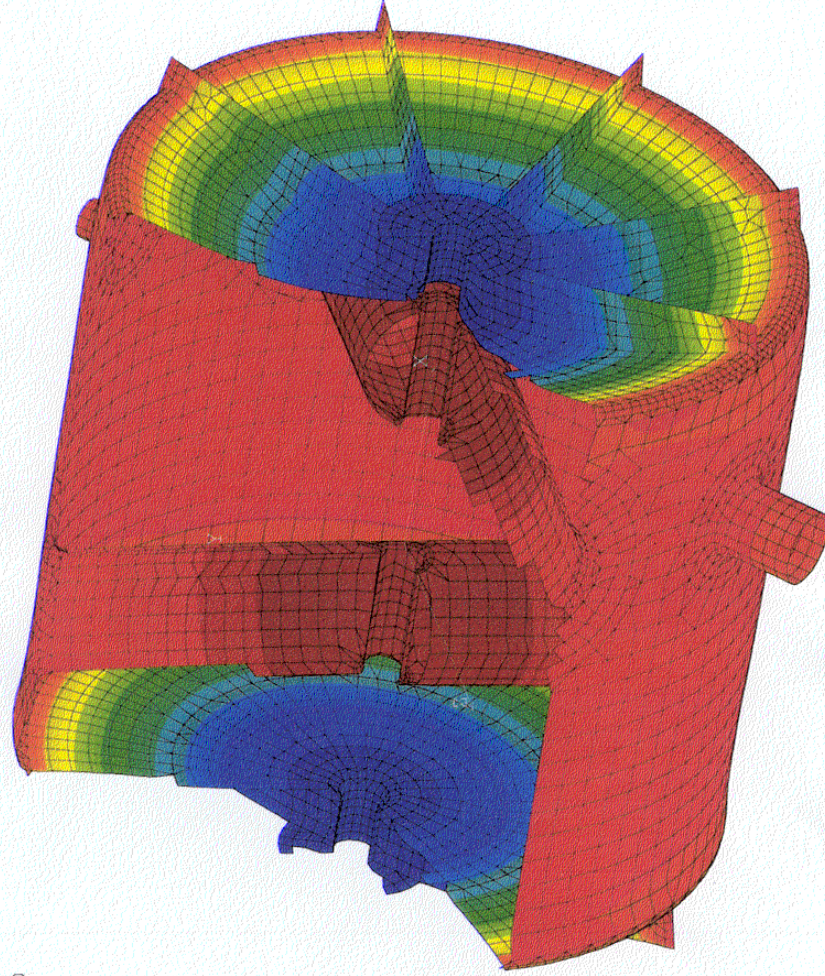
GEOMETRY PER ANL EB-24003-X
WITH WRAP-AROUND RADIAL ENDWALL STIFFENERS



F_Mode=1 291.962 Hz

FIGURE 6a
ANL 350 MHZ 3-GAP CAVITY
CASE 37 MODE 1 - AXIAL TRANSLATION
DISTORTIONS EXAGGERATED

Disp_Res
1.22570
1.07250
0.91926
0.76605
0.61284
0.45963
0.30642
0.15321
0.00000

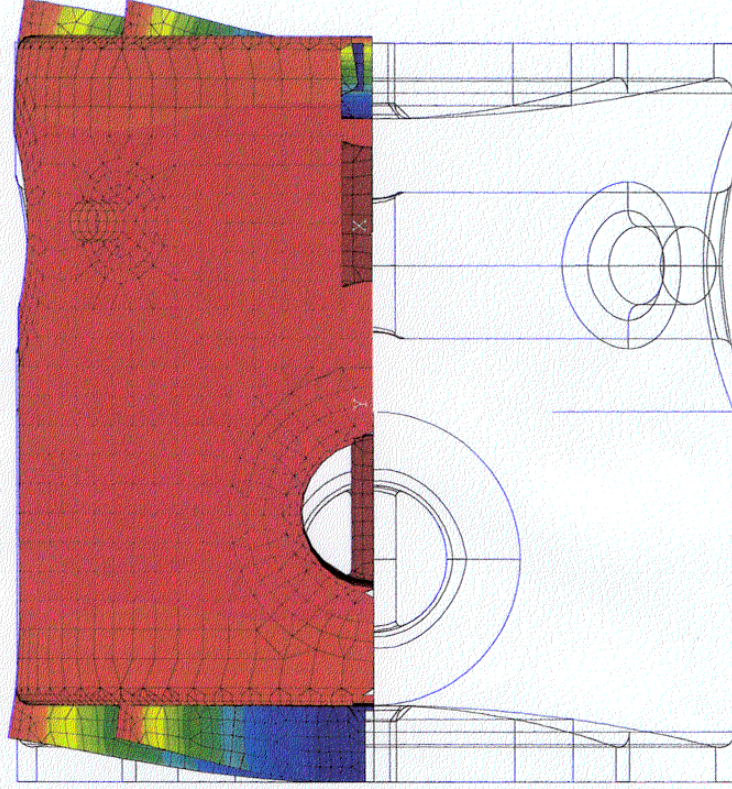
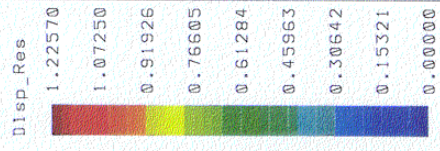


F_Mode=1 291.962 Hz

FIGURE 6b ANL 350 MHZ 3-GAP CAVITY

CASE 37 MODE 1 - AXIAL TRANSLATION

DISTORTIONS EXAGGERATED



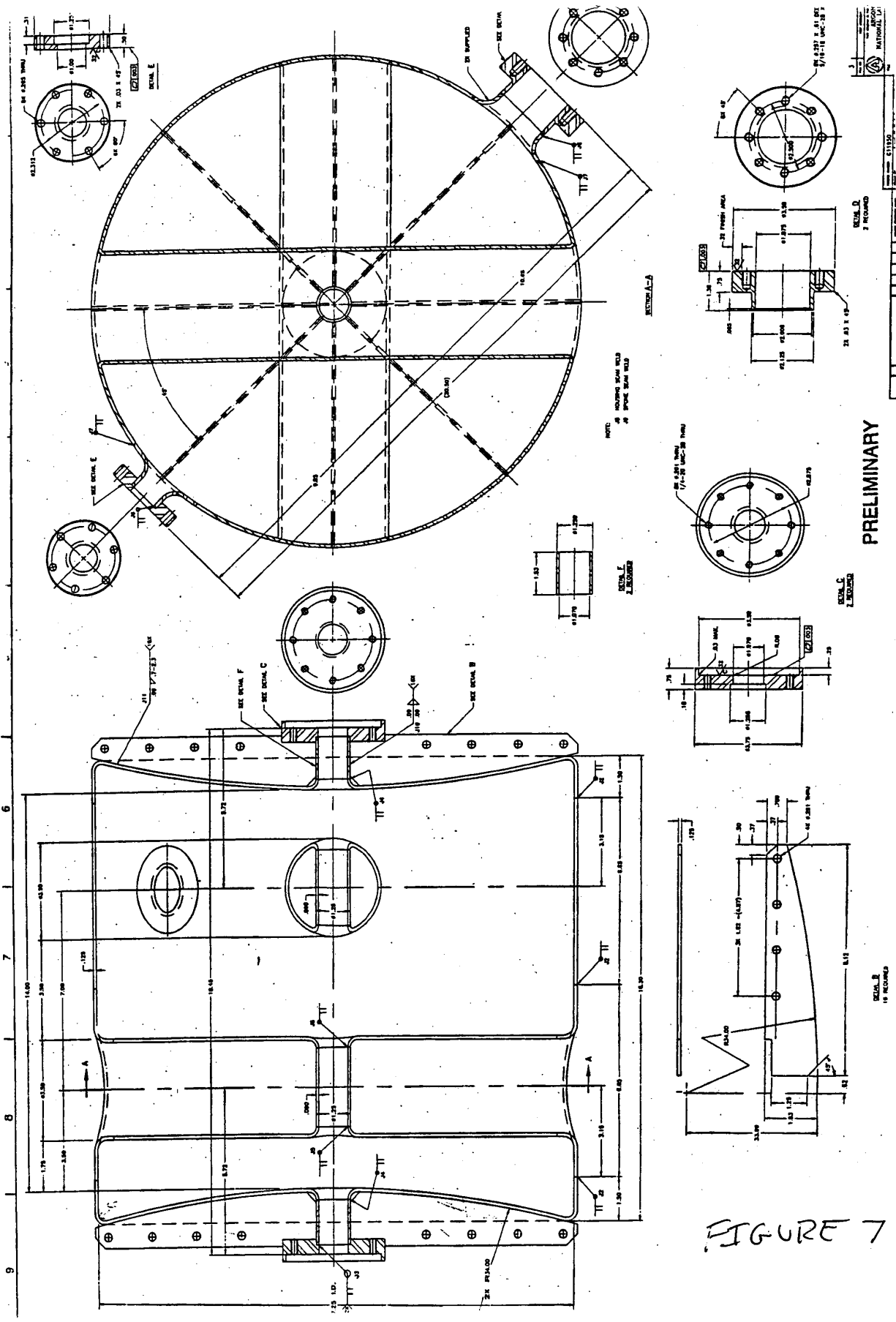


FIGURE 7

CC:

B. Baillie, LANSCE-1, MS H817
K. Bongardt, Forschungszentrum Jülich
D. Bruhn, LANSCE-1, MS H817
M. Cappiello, APT-TPO, MS H816
K. C. Chan, APT/TPO, MS H816
R. Garnett, LANSCE-1, MS H817
R. Gentzlinger, ESA-DE, MS H821
D. Gilpatrick, LANSCE-1, MS H817
H. Haagenstad, LANSCE-1, MS H817
W. B. Haynes, LANSCE-9, MS H851
A. Jason, LANSCE-1, MS H817
M. Johnson, Cornell Univ.
M. Kedzie, ANL
P. Kelley, LANSCE-1, MS H817
F. Krawczyk, LANSCE-1, MS H817
G. Lawrence, APT/TPO, MS H816
J. Ledford, LANSCE-1, MS H817
P. Leslie, LANSCE-1, MS H817
R. Lujan, LANSCE-1, MS H817
F. Martinez, LANSCE-1, MS H817
K. Meunier, Sunwest Cad
J. Mitchell, LANSCE-1, MS H817
D. Montoya, LANSCE-1, MS H817
D. Montoya, ESA-DE, MS N821
A. Naranjo, LANSCE-1, MS H817
J. O'Hara, Honeywell, MS H817
P. Ostronouv, ANL
N. Patterson, LANSCE-1, MS H817
H. Padamsee, Cornell Univ.
A. Rendon, LANSCE-1, MS H817
P. Roybal, LANSCE-1, MS H817
R. Roybal, LANSCE-1, MS H817
L. Rybarczyk, LANSCE-1, MS H817
E. Schmierer, ESA-DE, MS H821
S. Schriber, LANSCE-DO, MS H845
A. Shapiro, LANSCE-1, MS H817
R. Sheffield, APT-TPO, MS H816
K. Shepard, ANL
F. Sigler, LANSCE-1, MS H817
J. Szalczinger, LANSCE-1, MS H817
T. Tajima, LANSCE-1, MS H817
R. Valdiviez, LANSCE-1, MSH817
T. Wangler, LANSCE-1, MS H817
R. Wood, LANSCE-1, MS H817
T. Wright, LANSCE-1, MS H817
LANSCE-1 Reading File, MS H817